Sustainable Chemistry for Climate Action 2 (2023) 100011

Contents lists available at ScienceDirect

Sustainable Chemistry for Climate Action

journal homepage: www.elsevier.com/locate/scca

# Synthesis and characterization of lignin nanoparticles isolated from oil palm empty fruit bunch and application in biocomposites

Udari Prasadini Perera[a], Mei Ling Foo[a], Irene Mei Leng Chew[a,b,*]

[a] Chemical Engineering Discipline, School of Engineering, Monash University Malaysia, 47500 Bandar Sunway, Selangor, Malaysia
[b] Monash-Industry Plant Oils Research Laboratory (MIPO), Monash University Malaysia, 47500 Bandar Sunway, Selangor, Malaysia

ARTICLE INFO

*Keywords:*
Lignin nanoparticles
Ultrasonication
Alkali lignin
Starch composites
Biocomposites
Reinforcing agent

ABSTRACT

Valorisation of industrial biomass wastes, such as oil palm empty fruit bunch (EFB) generated by the palm oil industry, could promote its sustainable use while minimising the adverse impacts on the environment. To this end, the present study attempted to synthesize lignin from EFB. A simple yet environmentally friendly technique, ultrasonication, has been employed to convert the isolated lignin to lignin nanoparticles (LNPs). The transmission electron microscopy results and dynamic light scattering measurements have confirmed the mean particle size of LNPs at 220 nm. Also, LNPs showed better thermal performance compared to lignin, as indicated by a higher glass transition and maximum degradation temperature. LNPs were stable in the pH range of 4.5 - 9.0 and sodium chloride concentration below 100 mM over a week of storage. At pH 7, the LNP suspension remains stable without precipitation for up to three months of storage under ambient conditions. In addition, the LNPs were incorporated into the starch matrix to form biocomposites and then compared against lignin biocomposites and neat starch film for their thermal, mechanical, and hydrophobic performance. The biocomposites with LNPs are anticipatedly possessing better performance than the neat starch film and lignin biocomposites in all aspects.

## 1. Introduction

Biomass wastes generated as forestry residues, agricultural, and food waste have raised concerns about the environmental issues internationally [1]. In the Malaysian context, the palm oil industry has produced 47 million metric tons of dry biomass [2,3]. Typically, solid oil palm biomass waste consists of three components: empty fruit bunch (EFB, 53%), shell (29%), and fibre (18%) [4]. EFB consists of 33.5% cellulose, 21.5% hemicellulose, and 20.4% lignin [5]. Despite the high volume of EFB being generated every year, only a small fraction of EFB ends up as industrial products, such as pulp and fibreboard, and as a stabilising agent, whereas a large portion often gets left out as mulch [6,7]. The fibrous nature and high moisture content of EFB have been significant challenges for processing EFB into industrial products. Nevertheless, EFB could play an essential role as a source for biorefineries to produce bioethanol and value-added chemicals [8,9]. Many studies focused on converting EFB to bioethanol [2,10] or value-added products such as nanocrystalline cellulose [11,12]. Produced a high volume of lignin-rich alkali black liquor during the pretreatment processing. The alkali black liquor can be employed to isolate lignin using different techniques, such as acid precipitation and membrane separation. The isolated EFB-origin lignin has been used as UV stabilizers [13], antioxidant [14,15], corrosion inhibitor [16], biosorption for copper [17], phenol-formaldehyde production [18] and as an additive in polymer blends/composites [19]. However, challenges such as complex lignin structure, which depends on its origin and separation process, large and uneven particle sizes, water insolubility, undefined functional groups, poor dispersion, and weak reactivity, limit the performance of lignin, and hence, hindering the valorisation of EFB-lignin in these applications [20,21].

The nanoscale conversion of lignin has improved the lignin valorisation process efficiency [22]. Compared to lignin, lignin nanoparticles (LNPs) possess a higher surface-to-volume ratio and better dispersibility, leading to improved mechanical performance and thermal stabil-

*List of abbreviations:* $D_H$, Average hydrodynamic diameter; DI, Deionised water; DLS, Dynamic light scattering; DSC, Differential scanning calorimetry; DTG, Derivative thermogravimetric curve; EFB, Empty fruit bunch; FE-SEM, Field emission scanning electron microscope; FTIR, Fourier-transform infrared spectroscopy; LNPs, Lignin nanoparticles; NMR, Nuclear Magnetic Resonance; TEM, Transmission electron microscopy; TGA, Thermogravimetric analysis; Tg, Glass transition temperature; Tmax, Maximum degradation temperature; UV-vis, Ultraviolet-visible spectroscopy.

* Corresponding author.
*E-mail address:* irene.chew@monash.edu (I.M.L. Chew).

https://doi.org/10.1016/j.scca.2022.100011
Received 17 September 2022; Received in revised form 13 December 2022; Accepted 30 December 2022

ity [23–25]. Furthermore, LNPs also showed greater antioxidant activity [26,27] and good UV shielding properties [28,29]. Therefore, LNPs show promising potential in a broad range of applications such as Pickering emulsions [30,31], sunscreens [32], drug delivery [33], automobile applications [34,35] and as a filler/reinforcer for biocomposites [36–38].

Numerous methods have been adopted to synthesize LNPs, including producing colloids by self-assembly [39], dissolving lignin in an organic solvent and dialysis (solvent exchange) [40], acid precipitation [41–43], carbon dioxide saturation, aerosol processing [44,45], high shear /pressure homogenisation [24] and ultrasonication [20,46,47]. However, many LNPs preparation methods have limitations. For example, solvent exchange and acid precipitation are energy-intensive techniques with high consumption of solvents and water. Also, hazardous solvents such as toluene diisocyanate [48] and pyridine [49] and dichloromethane [50] were employed in some LNPs preparation methods. Moreover, some processes require surface modification of lignin, i.e. acetylation of lignin before disintegrating into the nanoscale, which usually involves consuming hazardous chemicals such as acetyl bromide [40]. On the contrary, ultrasonication requires no organic solvents or chemical modification on lignin and requires no post-treatment. During the ultrasonication, lignin particles may face both physical (ultrasound-induced acoustic cavitation, intense local heating and pressure) and chemical effects (generation of hydrogen and hydroxyl radicals, which tackle the functional groups available on a particle) that generate highly monodisperse nanoparticles [22]. Compared to the other methods, the overall preparation time of LNPS via ultrasonication is relatively short, i.e., one hour [46,51]. However, the economic feasibility of sonication depends on sonication time, frequency, the wattage of the sonicator, amplitude and lignin concentration. Long ultrasonication time, high frequency and amplitude, and low lignin concentration led to increased energy consumption. Hence, attention should be given to reducing ultrasonication time to make the process energy-efficient and sustainable. A summary of the earlier works of ultrasonication produced LNPs and LNPs of EFB-origin are presented in Table 1.

In this study, EFB-origin lignin was obtained through alkali pulping the EFB fibres, followed by the acid precipitation of black liquor. Then, the isolated lignin was disintegrated into LNPs using ultrasonication. The morphological, chemical and physical characteristics of lignin and LNPs and the stability of LNPs in different pH and salt conditions are studied. The LNPs were then incorporated into the starch biocomposites to investigate their performance as the reinforcing agent in terms of thermal, mechanical, and hydrophobic properties. To our knowledge, this is the first work presenting the preparation of EFB-derived LNPs using ultrasonication and the first study to produce starch composites with EFB LNPs.

## 2. Materials and method

### 2.1. Materials

EFB fibres were received complimentary from Eureka Synergy Sdn. Bhd. Sodium hydroxide (NaOH) and sulfuric acid ($H_2SO_4$, 95–97%) were purchased from Friedemann Schmidt Chemical. Glycerol (99% purity) and corn starch were supplied by Fisher Scientific and RM chemicals, respectively. All reagents were in analytical grade and used without further purification. Deionised water (DI) was used to prepare all aqueous solutions.

### 2.2. Lignin isolation

The alkali treatment was adapted from the preparation of cellulose by Foo et al. [55] with minor modifications to the process. Briefly, EFB fibres were ground using Pulverisette 14 (Fritsch) rotor mills until they passed through a 500 μm sieve tray (ASTM Standard). The sieved fibres were washed several times using DI water at 50 °C (fiber to liquid ratio of 1 g:30 ml used throughout the experiment) to remove water-soluble substances. Then the fibres were oven-dried at 60 °C until a constant weight was obtained. Dried fibres were treated with 4 w/v% NaOH solution at 80 °C for 6 h, with continuous stirring. After the treatment, fibres were filtered and washed with DI water until neutral pH was obtained. The resulting black liquor was filtered with Whatman filter paper (pore size = 11 μm) to remove degraded carbohydrates and inorganic salts. Lignin separation was carried out by acidifying the black liquor to pH 2 by gradually adding 20 v/v% $H_2SO_4$ solutions. The suspension was then centrifuged at 11,000 rpm for 15 min to separate the lignin particles, which were later collected and washed with 0.001 M $H_2SO_4$. Both acidification and washing steps were carried out under constant stirring. Again, the suspension was centrifuged (11,000 rpm, 15 min) to separate lignin from the acidic solution. The isolated lignin was freeze-dried at −95 °C for 24 h and ground to powder form using a motor and pestle. The stock lignin powder was stored in an airtight, dark colour glass bottle for further processing and characterisation.

### 2.3. Synthesis of lignin nanoparticles

Lignin powder was suspended in water using continuous stirring. The initial pH of the lignin suspension was pH 2–4, which was adjusted to around pH 7 using a diluted NaOH solution (0.001 M). The neutralised lignin suspension (0.5 wt%) was then sonicated at 60% amplitude using a probe sonicator (QSONICA Q700, 20 kHz, 700 W) to obtain LNP. The samples were subjected to an ultrasonication duration of up to 2 h to study the effect of ultrasonication time on particle size. The samples were kept inside an ice bath to prevent heat-

**Table 1**
Earlier works of ultrasonication-assisted synthesis of lignin nanoparticles and empty fruit bunch origin lignin nanoparticles.

| Biomass source | Synthesis method | Morphology | Application | Reference |
|---|---|---|---|---|
| Softwood kraft lignin | Ultrasonication for 6 h. (20 kHz, 130 W, 95% amplitude, 0.1 wt% lignin) | 10–50 nm, irregular shape | Polyurethane biocomposites | [20] |
| Wheat straw lignin & Sarkanda grass lignin | Ultrasonication for 1 h. (20 Hz, 600 W, 0.7% lignin) | 0.01–0.05 μm, irregular shape | N/A | [47] |
| Alkali Lignin | Ultrasonication for 1 h (25 kHz., 800 W, 16% w/v lignin) | 200 nm, non-spherical | Nanocomposite hydrogel for biomedical applications | [46] |
| Lignin from giant reeds (Arundo donax) | Ultrasonication | 10–50 nm, irregular | Nanocomposite for food packing | [23] |
| EFB | Homogenisation (10,400–12,400 rpm for 1 h, 1 wt% lignin) accompanied by 10 min of ultrasonication | ~50 nm, rough surface | Emulsifier | [52] |
| EFB | High-Pressure Homogenisation | ~283 nm irregular | N/A | [24] |
| EFB | Homogenisation (6400- 12,400 rpm for 1 −4 h) | 20–130 nm, irregular | Emulsifier | [53] |
| EFB | Ball Milling (170 rpm for 24 h) | 38–106 nm, irregular | Bioplastic films with *Kappaphycus alvarezii* | [54] |
| EFB | Ultrasonication (0.5 wt%, 30 min, 20 kHz, 700 W) | ~220 nm | Biocomposites with starch | This work |

induced damage to the samples due to the excessive heat generated during the ultrasonication process. A small volume of lignin suspension was taken from the sonicating sample every 30 min for particle size measurement. After optimising the ultrasonication time for the synthesis of LNP, the samples were subjected to freeze-drying before characterisation.

### 2.4. Characterization of lignin nanoparticles

#### 2.4.1. Particle size distribution

The average hydrodynamic diameter (avg. $D_H$) of LNPs was examined using the dynamic scattering method (DLS) with a Malvern Nano-ZS Zetasizer (Malvern Instruments). For zeta potential measurements, the Smoluchowski model was applied to electrophoretic mobility. All measurements were performed in triplicate.

#### 2.4.2. Electron microscopy

The particle size and structure of LNPs were observed by transmission electron microscopy (TEM, Tecnai G2 20S-TWIN) operating at 200 kV. The diluted LNP suspension was dropped onto a carbon-coated copper grid and dried at room temperature before visualisations with TEM. The morphology of lignin was visualised using a field emission scanning electron microscope (FE-SEM; SU8010, Hitachi) with an acceleration voltage of 5 kV. The samples were platinum coated to improve the conductivity of the sample.

#### 2.4.3. Fourier transform infrared spectroscopy (FTIR)

The infrared spectra of freeze-dried lignin and LNP samples were recorded using the Thermo-Nicolet iS10 (Thermo Fisher Scientific) spectrophotometer equipped with an ATR diamond probe accessory over the range of 400 – 4000 $cm^{-1}$ with an accumulation of 64 scans.

#### 2.4.4. Ultraviolet-visible (UV–vis) spectroscopy

UV–vis spectra of lignin and LNPs were recorded on a spectrometer (Cary 100, Agilent) in the range of 200 – 800 nm. The deionised water was used as a blank sample. Three measurements were performed for each sample, and its average value was presented in the graphs.

#### 2.4.5. Nuclear magnetic resonance (NMR)

The chemical composition of LNPs was determined using $^{13}C$ NMR according to the procedure proposed by Balakshin and Capanema, [56]. The NMR spectra of samples were obtained from a Bruker UltraShield 300 MHz spectrometer. Briefly, the sample was weighed accurately to 100 mg and was dissolved in 0.5 mL of dimethyl sulfoxide-d6 (DMSO-$d_6$) containing a relaxation agent, chromium (III) acetylacetonate and internal standard (IS), trioxane. About 20,000 scans were collected. The $^1H$ NMR analysis was carried out using a Bruker UltraShield 300 MHz spectrometer, and DMSO-$d_6$ was used as a solvent.

#### 2.4.6. Thermogravimetric analysis (TGA)

Thermogravimetric analysis was performed with a thermogravimetric analyser (Q50, TA instruments). 10 mg of the sample was heated in the nitrogen environment from 25 to 800 °C at a ramping rate of 10 °C $min^{-1}$. The $T_g$ values of lignin and LNPs were obtained by analysing the second scan (reheat from – 20 to 210 °C) with "TRIOS" software.

#### 2.4.7. Differential scanning calorimetry (DSC)

DSC scans were performed with a TA Instruments DSC Q200 (TA Instruments). Approximately 5 mg of the sample was placed in a sealed sample pan and equilibrated to −20 °C. The sample was heated from −20 to 210 °C at a heating rate of 10 °C $min^{-1}$ under a nitrogen atmosphere.

**Table 2**
Composition of lignin/ lignin nanoparticle films.

| Film Name | Lignin wt. (%) | LNPs wt. (%) |
|---|---|---|
| NT (Neat) | 0 | 0 |
| 2L | 2 | 0 |
| 4L | 4 | 0 |
| 2NL | 0 | 2 |
| 4NL | 0 | 4 |

#### 2.4.8. Lignin nanoparticles suspension stability

LNP suspensions of 0.2 wt% were prepared to investigate the effects of pH and salt concentrations on the stability of samples in terms of the changes in particle size and zeta potential. The pH of the LNP suspension was adjusted to pH 1.5 using 100 mM HCl and pH 12 using 100 mM NaOH solutions. In separate experiments, LNP suspensions with 1 mM, 10 mM, 100 mM, 500 mM and 1 M NaCl were prepared at the neutral pH. The samples with different pH and salt concentrations were sonicated for 30 min at 60% amplitude. The particle size and zeta potential of samples after being subjected to different pH's and salt concentrations were determined using the Zetasizer for 0- and 7-day storage at room temperature.

### 2.5. Preparation of lignin nanoparticle composites

The composite films were prepared using the solvent casting method. For the reference neat film, 10 g of starch and 5 g of glycerol were disposed of in 185 g of DI water. The mixtures were heated to 90 °C with continuous stirring. Once the solution reached 90 °C, it was kept at the same temperature with continuous stirring for 5 min. Then, the resulting gelatinized suspension was sonicated for 10 min at 60% amplitude. After the ultrasonication, the suspension was poured into the Petri dishes and then oven-dried at 45 °C for 24 h. The same procedure was applied to lignin and LNP biocomposites films. The amount of lignin/LNPs added to the biocomposites were given in Table 2.

### 2.6. Characterization of composites

The biocomposite films were subjected to TGA and DSC analysis based on the same procedure mentioned in Sections 2.4.6 and 2.4.7, respectively.

#### 2.6.1. Contact angle

The hydrophobicity of samples was determined using a goniometer (Ramehert) equipped with a computer-automated program. The films were fixed on glass plates with double-sided adhesive tape. 4 μL of a water droplet was placed on the surface of the film with an auto pipette, and the images were captured immediately. The contact angle was determined using DROPimage based on the sessile drop technique. The first ten contact angles were taken on three different positions of the film, and the mean value was reported.

#### 2.6.2. Mechanical performance

The mechanical properties of the films were evaluated by a texture analyser, TA-XT2 (Stable Micro Systems), using the tensile grip. Rectangular samples (40 mm × 12.5 mm) were tested with crosshead speed and distance of 1.00 $mms^{-1}$ and 40 mm, respectively. A 5 kg load cell was used, and the initial gauge length of 25 mm was set. Three specimens from the same sample were tested, and their average value was stated.

## 3. Results and discussion

The amount of lignin isolated from EFB black liquor was about 11% on a dry weight basis. The lignin contained 89.5% acid-insoluble lignin

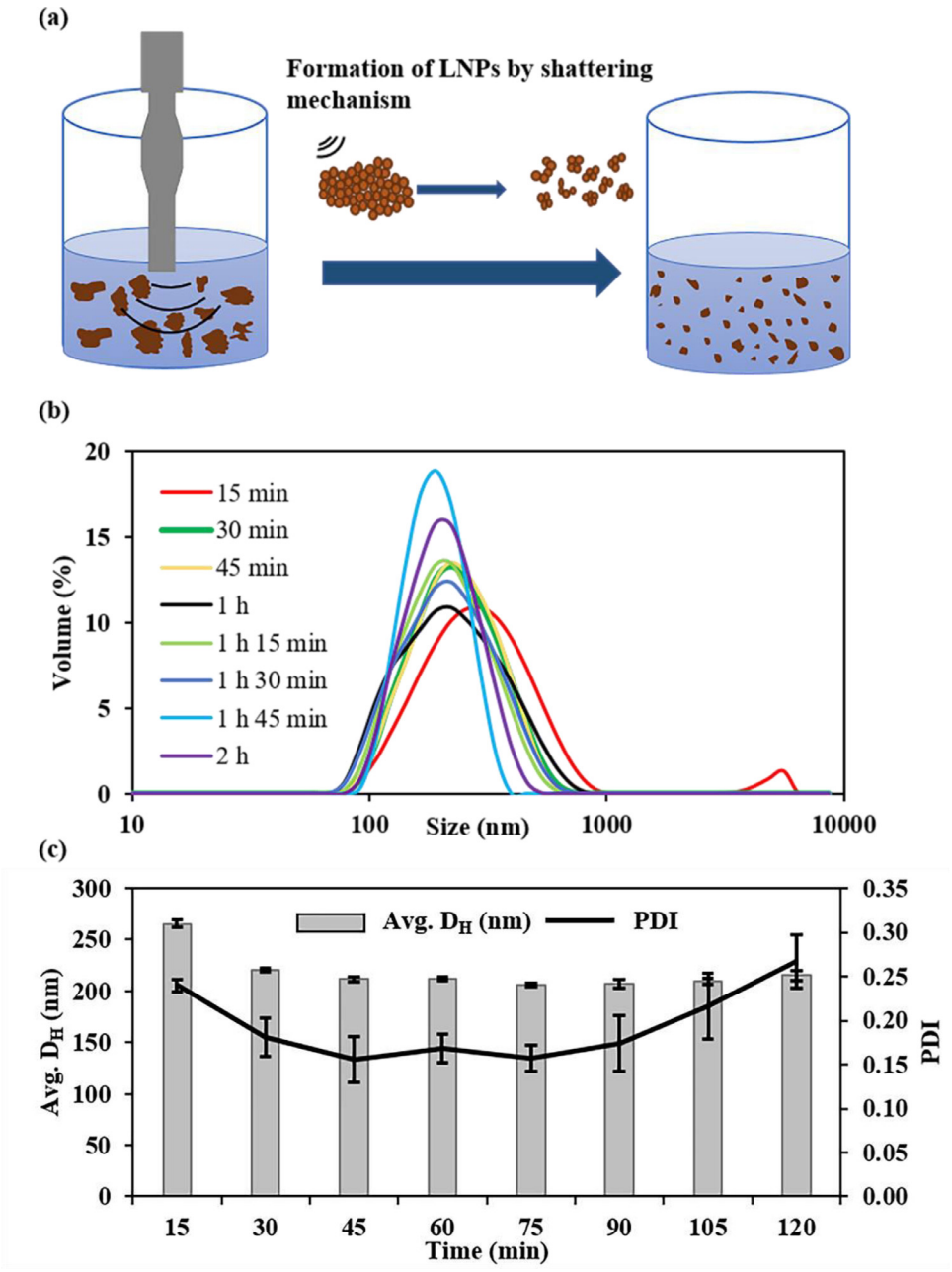


**Fig. 1.** (a) Schematic diagram of lignin size reduction by ultrasonication [47]., (b) Lignin nanoparticles (LNP) size distribution by volume for different ultrasonication times, (c) Effect of sonication time on LNP particle size and Polydispersity Index (PDI). The average value of triplicate measurements was presented as means ± standard deviation.

(Klason) and 4.31% acid-soluble lignin. The yield of the NL synthesised with ultrasonication was about 81% (dry weight basis). Please refer to the supporting information for the detailed analysis of isolated lignin characterisation. These results are similar to the previously reported NMR results on EFB-origin lignin and proved that EFB-origin lignin contains mainly syringyl, guaiacyl and p-hydroxyphenyl lignin monomers (SGH lignin) [57].

### 3.1. Formation of lignin nanoparticles and effect of ultrasonication time

Fig. 1(a) illustrates the synthesis process of LNPs from lignin via the ultrasonication process. The high energy generated by ultrasonication results in particle shattering and disintegrating the lignin agglomerates into several small fragments on the nanoscale in a single event (similar observations have been reported in [58]). The DLS results of LNP samples were presented in Fig. 1(b). A bimodal distribution was observed when the sample was sonicated for 15 min, in which the distribution peaks were found around 360 nm and 5068 nm. Increasing the ultrasonication duration to 30 min has led to a mono-modal distribution. A narrower LNP size distribution was observed with increased ultrasonication time due to the shattering effect of ultrasonication.

The avg. $D_H$ reduced from 270 nm to 220 nm when the ultrasonication time increased from 15 to 30 min (Fig. 1(c)). The $D_H$ of LNP was further reduced to 211 nm after 45 min ultrasonication. However, further prolonged ultrasonication time caused negligible changes to the $D_H$ and resulted in a $D_H$ of 215 nm when the ultrasonication time increased to 120 min. The polydispersity index (PDI) of lignin suspension was 1.00 before the ultrasonication. It was decreased to 0.16 – 0.27 after the ultrasonication (higher PDI indicates higher polydispersity in particle sizes). A longer ultrasonication time has caused the PDI to reduce gradually, and the minimum PDI value was obtained at 45 min of ultrasonication. Nevertheless, no clear trend was observed in PDI when the ultrasonication time was beyond 45 min.

Fig. 2(a) shows the morphology of lignin isolated from EFB. Before ultrasonication, the lignin particles were irregular and agglomerated as micron particles in 2–5 μm. The agglomeration results from strong in-

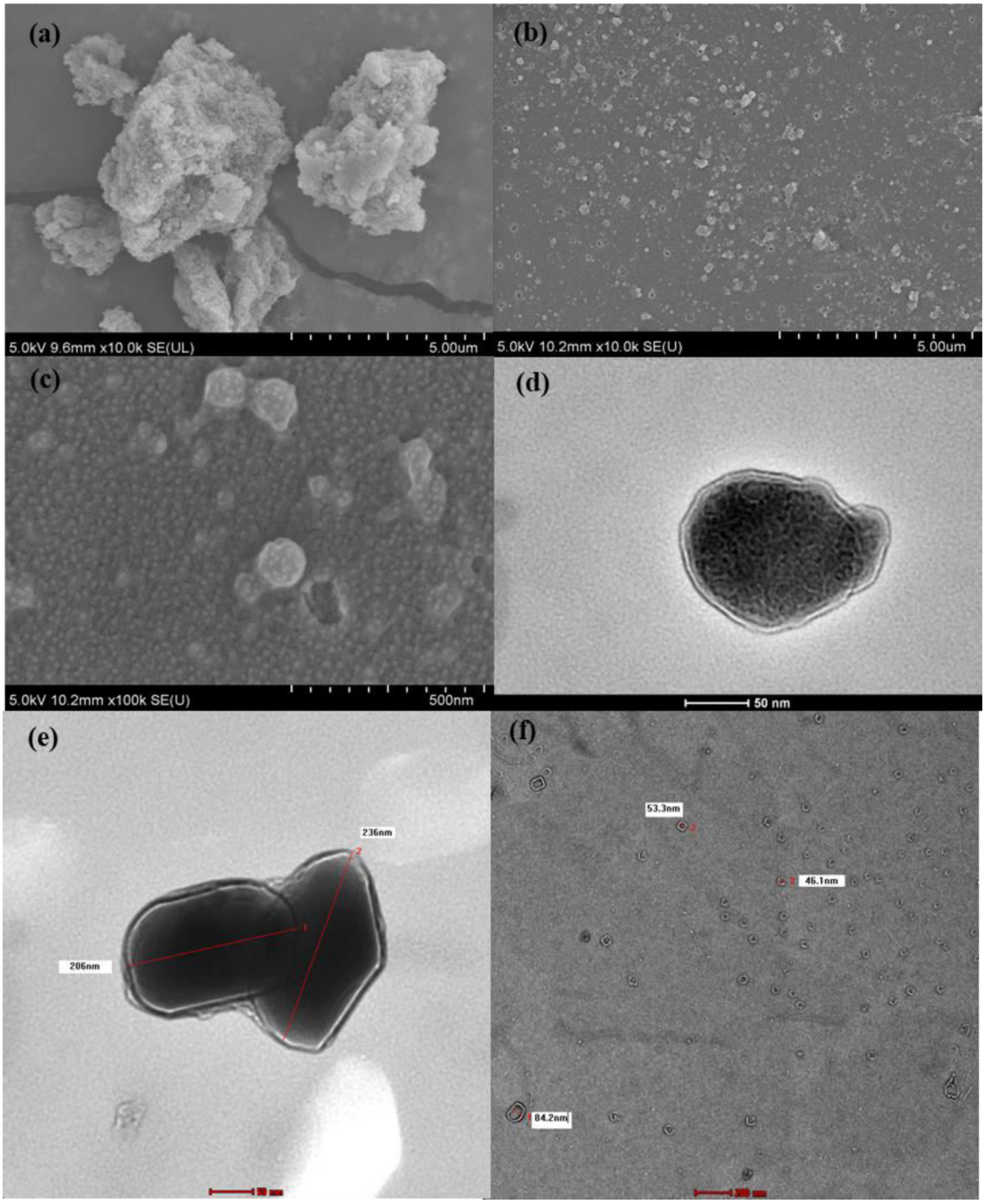


**Fig. 2.** Scanning electron microscopy images of (a) lignin, (b) and (c) lignin nanoparticles, and (d-f) transmission electron microscopy images of lignin nanoparticles.

termolecular hydrogen bonding between macromolecular lignin [59]. Ultrasonication successfully disintegrated the lignin from the micrometre range to ~200 nm (Fig. 2(b-d)).

### 3.2. Structural analysis of lignin and lignin nanoparticles

FTIR was used to compare the chemical structure of lignin and LNP, and the results are presented in Fig. 3(a). The absorbance peaks at 3350 $cm^{-1}$ and 2900 $cm^{-1}$ correspond to the total hydroxyl groups and C–H stretching in methyl, methylene, and methoxyl groups, respectively [60]. The weak signal observed at 1700 $cm^{-1}$ was ascribed to the C=O stretching of carbonyl moieties of hemicellulose impurities (i.e., conjugated aldehydes and carboxylic acid) that could be present in lignin. This peak was missing in the spectra of LNP, which could be due to the oxidation of hemicellulose impurities during ultrasonication [20].

An additional shoulder at 1643 $cm^{-1}$ was noted in LNP spectra, which could be attributed to carbonyl stretching vibrations of intramolecular hydrogen-bonded acrylic acid. In addition, Garcia Gonzalez et al. [61] suggested that these intramolecular hydrogen bonds may be formed during the partial oxidation of lignin during the ultrasonication process. The hydrogen bonds could improve the dispersion stability of LNPs in polar solvents due to the lowered interparticle attractions. No significant differences between lignin and LNP were noticed in the aromatic region (1610 $cm^{-1}$ to 1505 $cm^{-1}$), which implied less or no ultrasonication impact on the area. Similarly, the following peaks were unaffected by ultrasonication; 1458 $cm^{-1}$ (O–H in-plane bending), 1420 $cm^{-1}$ (aromatic ring vibration combined with C–H in-

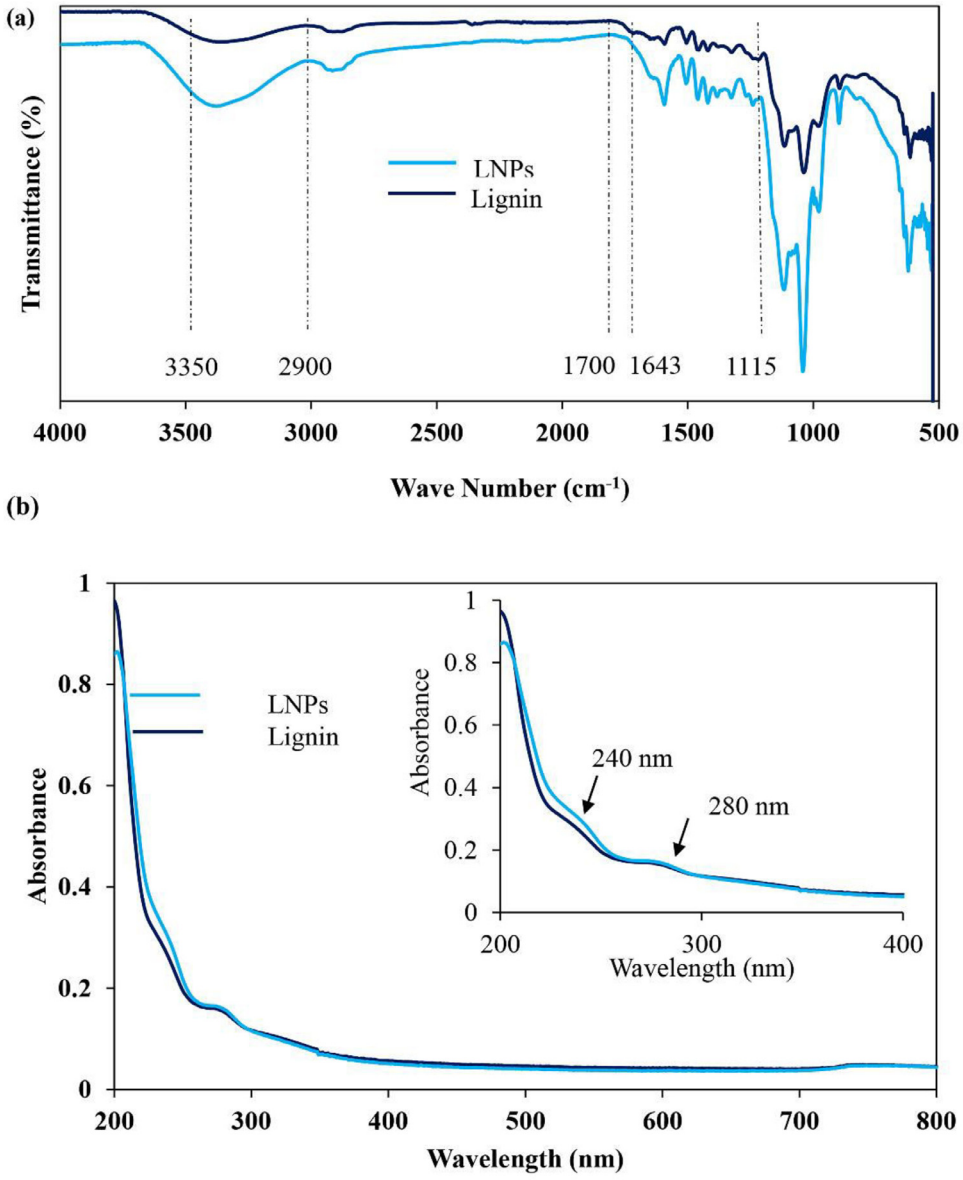


**Fig. 3.** (a) Fourier-transform Infrared spectra and (b) ultraviolet-visible spectra of lignin and lignin nanoparticles (LNPs).

plane vibration), 1321 $cm^{-1}$ (Bending vibration of C–H and C–O bonds) and 1230 $cm^{-1}$ (C–O–C bond) [62]. Both spectra showed a peak at 1115 $cm^{-1}$, assigned to condensed phenolic groups [47].

The elucidation of lignin and LNP structures were qualitatively determined using UV–vis spectroscopy. The spectrums of lignin and LNPs have been presented in Fig. 3(b), where the inset is the enlarged part of the wavelength in the range of 200–400 nm. Both frequencies showed a shoulder area with identical absorbance values around 300–350 nm, a characteristic absorbance of the conjugated moieties, i.e., $\alpha$-carbonyl groups [20]. The absorbance at 280 nm corresponded to the $\pi$-$\pi$ transition of guaiacyl structural units in lignin [63]. In general, lignin and LNPs were found to have a similar wavelength and absorbance values. However, the absorbance at 240 nm corresponded to nonconjugated phenolic groups in LNP [64]. It has a higher absorbance peak than lignin, indicating a higher phenolic hydroxyl amount, and this finding further validated the FTIR results.

### 3.3. Thermal properties of lignin nanoparticles

The graphs reflecting the thermal degradation behaviours of lignin and LNP are presented in Fig. 4. The thermogravimetric (TG) and derivative thermogravimetric (DTG) curves of lignin and LNPs are illustrated in Fig. 4(a). Lignin was noted with four steps of thermal degradation, while LNPs had three phases.

Both samples showed the initial weight loss peak ($T_{DTG\ max\ 1}$) at 52 °C due to the loss of absorbed water [65], and the weight loss was around 10%. The maximum thermal decomposition peak (second peak) of lignin at 229 °C was shifted to 285 °C for LNPs, indicating better thermal stability of LNPs. The weight loss between 150 and 250 °C could be due to the elimination of formic acid, formaldehyde, carbon dioxide and water resulting from the degradation of phenylpropane side chains [66]. Most of the weight loss (~30%) occurred for both samples in the temperature range of 275–500 °C due to the degradation of the lignin structure [67]. In this temperature region, monomeric phenols would be released into the vapour phase due to the fragmentation of inter-unit linkages of phenolic hydroxyl, carbonyl groups, benzylic [64] and hydroxyl [68,69]. LNPs had marginally lower thermal stability than lignin in this temperature range (275–500 °C), which could be caused by a higher surface-to-volume ratio of LNPs [70].

The third peak for lignin occurred at 340 °C, which associates with carbohydrates decomposition [64,71]. The absence of this peak in LNPs indicated a lack of hemicellulose in the sample compared to lignin, as

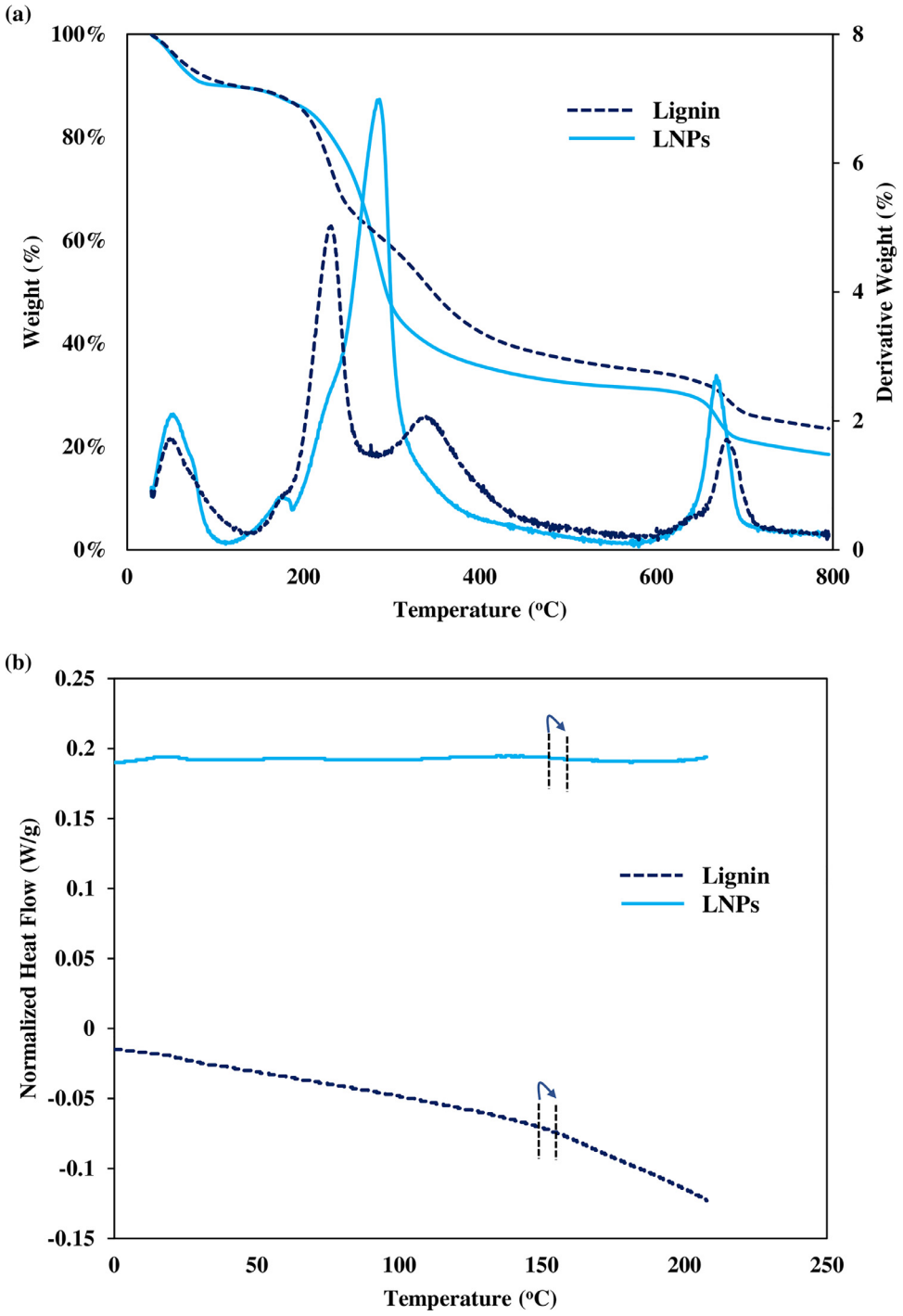


**Fig. 4.** (a) Thermogravimetric curves and (b) differential scanning calorimetry second scan curves of lignin and lignin nanoparticles (LNPs).

the ultrasonication effectively removed hemicellulosic impurities from lignin by cleaving the lignin-carbohydrate linkage [72]. Methoxy groups were decomposed at a temperature range of 400–600 °C, while the disintegration of C=O and C–O–C bonds occurred above 600 °C [73]. The final peak occurred around 675 °C for both samples, and the weight loss from 420 to 800 °C was around 16% for LNPs and lignin. The weight remained at 800 °C, attributed to non-volatile solids associated with highly condensed aromatic structures and the ash in lignin [67,65]. The final LNP residue (19%) was slightly lower than the lignin residue (24%).

Glass transition temperature ($T_g$) is essential to evaluate the feasibility of employing lignin and LNPs as precursors or fillers of composite material. $T_g$ is a direct indication of the mobility of the macromolecular chain, which can be influenced by many parameters such as molecular weight, chemical/physical crosslinking, and the presence of strong intermolecular bonds (i.e., Hydrogen bonding) [20]. Generally, the $T_g$ values of unmodified lignin fall into 90 to 180 °C [74]. The DSC was used to obtain $T_g$ (Fig. 4(b)) for lignin and LNPs. The slightly higher $T_g$ temperature for LNPs (156 °C) compared to lignin (154 °C) implied that ultrasonication had improved the thermal stability of lignin through size reduction. This finding is in close agreement with previous studies [24,75].

### 3.4. Stability of lignin nanoparticles

The stability of LNPs in different environments is vital to allow their potential application in various fields. The pH value and salt concentration are two such factors that affect nanoparticle stability. Hence, the stability of LNP dispersion was evaluated at different pH and salt

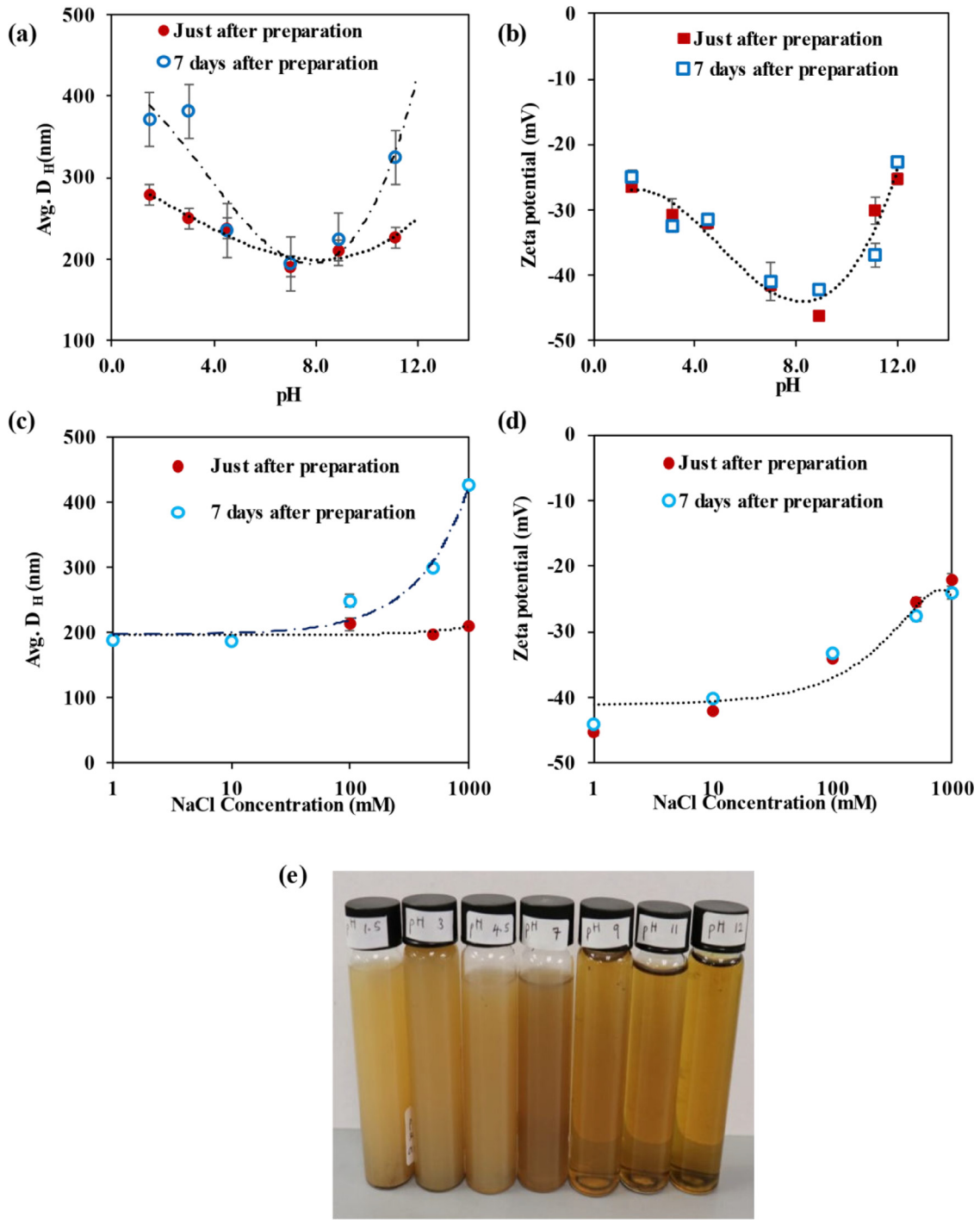


**Fig. 5.** Effect of pH on (a) Average hydrodynamic diameter ($D_H$) and (b) zeta potential of lignin nanoparticles (LNPs). The effect of salt concentration on (c) $D_H$ and (d) zeta potential of LNPs. The opaqueness (e) of LNPs at different pH (from left pH 1.5, 3.0,4.5, 7.0, 11.0 and 12.0). The average value of triplicate measurements was presented as means ± standard deviation.

concentrations. As demonstrated in Fig. 5(a), LNPs synthesised at pH 7.0–9.0 showed the smallest average hydrodynamic diameter ($D_H$) and insignificant change in size after a week of storage. LNPs at an extreme pH (below pH 4.5 and above pH 9.0) had a larger $D_H$ and significant size increment upon storage. This behaviour was caused by the aggregation (at pH below 4.5) and dissolution (at pH above 9.0) of LNPs particles [40,76], which was reflected in the appearance of the resulting suspensions. At low pH, the LNP suspensions were cloudy, whereas a darker but relatively more transparent appearance was observed in LNP suspensions at high pH (Fig. 5(e)) [77].

Zeta potential values of LNPs at different pH conditions are shown in Fig. 5(b). In general, zeta potential from 0 to ± 5 mV indicates the coagulation or flocculation, ±10 mV to ± 30 mV indicates the development of instability, and more than ± 30 mV represents stability as the suspension has sufficient repulsion energy to prevent aggregation [78,79]. Hence, LNP suspensions can be categorised into the stable region (pH 4.5–9.0, above |30 mV|) and incipient instability region (below pH 4.5 and above pH 11.0, below |30 mV|). The LNPs suspension was stable in the pH 4.5–9.0 region for a week with no considerable change in $D_H$ and zeta potential values. Hence, it is essential to adjust the pH of the lignin

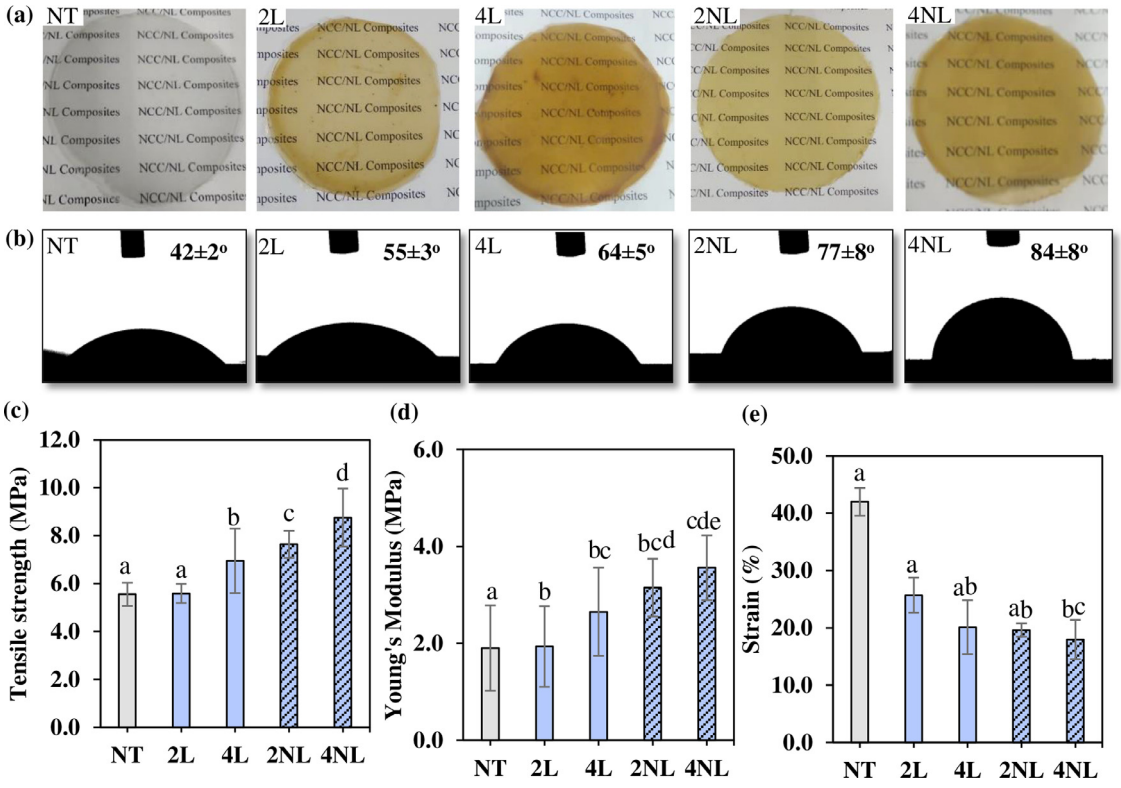


**Fig. 6.** (a) Digital images, (b) contact angle images (average values of hundred measurements were presented as means ± standard deviation), (c) tensile strength, (d) Young's modulus, and (e) strain of neat and composite films. (c-d: The average value of three measurements was presented as means ± standard deviation for mechanical properties. Different letters (a to e) denote statistical significance ($p < 0.05$) between means).

solution (initial pH 3.0–4.0) before ultrasonication to produce smaller LNPs with better stability. The $D_H$ and zeta potential of LNP suspension prepared at pH 7 was examined after three months of storage. It was found to be very stable ($D_H$ of 196.2 ± 3.61 nm and zeta potential at −41.16 ± 2.56 mV) without a noticeable difference in both $D_H$ and zeta potential. This demonstrated the excellent stability of sonicated EFB-origin LNPs in water.

The influence of NaCl concentration on the $D_H$ and zeta potential of LNPs is presented in Fig. 5(c) and (d). With the increment of NaCl concentration, the $D_H$ of LNPs increased while the absolute zeta potential value reduced. Above 100 mM NaCl concentrations, zeta potential dropped below |30|mV (−25.5 and −22.1 mV for 500 mM and 1000 mM, respectively). The $D_H$ increased dramatically after a week of storage due to the aggregation. The addition of salt into colloidal dispersions generally directs the screening of electrostatic interaction between particles [80,76]. Initially, LNPs had a zeta potential of around −40 mV (at pH 7. 0 mM NaCl) due to the electrical double layer formed by the surface charge of the phenolic hydroxyl groups and carboxyl groups [40]. When positively charged sodium ions were added to LNPs suspension, they accumulated around the LNPs particles and thinned the electrostatic double layer. Consequently, van der Waal's forces become governing, and the particle may aggregate. This effect becomes more potent at high NaCl concentrations, as indicated by the lower absolute zeta potential value and increased $D_H$.

### 3.5. Properties of biocomposites

Fig. 6(a) shows the digital images of neat, lignin, and LNP composite films. It can be seen that neat film exhibited the highest optical transparency. With the increase of lignin/ LNPs load, the films turned darker, and the words under the films became less clear. Generally, a good colour consistency indicates a uniform dispersion [81]. Both 2 L and 4 L films displayed a heterogeneous distribution of colour, probably due to the large particle size of lignin. This heterogeneity of colour was reduced in films containing LNPs, and the transparency of 2NL and 4NL films is higher than their respective lignin films. These results indicated that LNPs have better dispersion compared to lignin in composite films

The water contact angle measurements are useful to study the wetting behaviour and surface hydrophobicity of the polymer composites. Fig. 6(b) shows the contact angle measurements of neat and composite films. The contact angle of the neat film was 42° indicating the hydrophilic nature of starch due to the large number of hydroxyl groups present in starch [82]. With the addition of 2% lignin, the contact angle improved to 55°, as expected due to the hydrophobic nature of lignin. Increasing the lignin load to 4% resulted in a higher contact angle at 64° as the hydrophobicity of the compound improved. Generally, surface texture with micro/nanofillers is favourable in promoting surface hydrophobicity [83]. This was confirmed by the relatively higher contact angle of the 2NL film (77°) than 2 L and 4 L. The contact angle raised to 84° with the addition of 4% LNPs. These results indicate that the contact angle is enhanced with the additive load, and the LNPs have superior performance over lignin in intensifying hydrophobicity for starch composites.

The mechanical properties of neat and composite films are presented in Fig. 6(c to d). Both tensile strength (Fig. 6(c)) and Young's modulus (Fig. 6(d)) increased with the loading of lignin/ LNPs. The average tensile strength and Young's modulus of the neat film were 5.5 and 1.9 MPa, respectively. The addition of 2 wt% lignin increased the tensile strength slightly by 5.5%, and it further improved to 25.2% for 4 L film. As expected, LNP films had better mechanical performance than lignin films in tensile strength and Young's modulus. It was attributed to the nano-reinforcement and better dispersion of LNPs. The 4NL film showed the highest tensile strength at 8.8 MPa and Young's modulus of 3.6 MPa, 57.7% and 87.3% improvement compared to the neat film's tensile strength and Young's modulus, respectively. Furthermore, the composite films resulted in a significantly lower strain% compared to

**Table 3**
Thermal characteristics of composite films.

| | Tmax (°C) | Residue at 800 °C (%) | Tg (°C) |
|---|---|---|---|
| NT | 303.58 ± 1.92 [a] | 7.00 ± 0.05 [a] | 40.33 ± 0.75[a] |
| 2L | 306.79 ± 0.98 [a] | 8.06 ± 0.45 [ab] | 42.23 ± 0.59[a] |
| 4L | 307.12 ± 0.62 [a] | 9.12 ± 0.14 [b] | 48.44 ± 0.44[b] |
| 2NL | 308.22 ± 0.19 [a] | 8.89 ± 0.09 [b] | 58.00 ± 1.10[c] |
| 4NL | 287.10 ± 2.66 [b] | 11.79 ± 0.21 [c] | 60.75 ± 1.42[d] |

the neat film (Fig. 6(e)). The neat film had a strain% of 42%, whereas both LNPs and lignin films reduced the strain% by half. The difference in strain% between lignin and LNP films are less significant. However, the films that contained LNPs yielded a lower strain% than lignin film. A strain% of 25.7–20.1% was obtained for lignin film, whereas LNPs resulted in a strain% of 19.6–17.9%. Similar behaviour of tensile strength and young's modulus increment, while a reduction in elongation at break was observed by [84] in starch composites reinforced with Lignin–Cellulose Nanofiber. Also, Wang et al. [85] noticed the reduction of elongation upon the addition of the cellulose-lignin nanofibers to the polylactic acid. Lignin is generally considered a brittle material, and adding lignin particles may increase the brittleness of the composite [86]. Decreasing the elongation at break may cause in the reduction of composite toughness. Adding suitable bio-based crosslinker such as citric acid to the current composite toughness reduction could be prevented [87].

The effect of lignin and LNPs on the thermal stability of composite films were studied using TGA and DSC. The essential parameters, such as maximum degradation temperature ($T_{max}$), residue weight at the end of TGA analysis and $T_{g,}$ are given in Table 3. The maximum degradation temperature of the neat film was increased for 2 L, 4 L and 2NL films. However, 4NL film showed the lowest $T_{max}$ at 287 °C, much closer to LNP's actual maximum degradation temperature (285 °C). The similarity between starch and lignin degradation temperatures and the high amount of LNPs could be the reason behind the above observation [88].

Conversely, 4NL films showed the highest weight percentage of residue at 11.79% and a $T_g$ of 60 °C. Both residue weight and $T_g$ were improved with lignin and LNPs addition. Phenolic OH of lignin and Aromatic char formed from lignin at high temperature improved the thermal stability of the composites [89]. However, films containing LNPs showed better overall thermal performance than lignin films which could be attributed to the smaller size of LNPs and homogeneous dispersion in the starch matrix [38].

Starch is chosen for this study considering its abundance, low cost, and minimal requirements for modification. Apart from starch, LNPs have been added to other biodegradable polymers, including Poly (vinyl alcohol) (PVA) and poly(lactic acid) (PLA), to develop composites suitable for packaging. PVA is widely used as a polymer matrix to develop composites with high UV absorbing ability [90]. However, there could be compatibility issues with PVA and LNP, and surface modification of LNPs would be required to improve the compatibility. Similarly, PLA is utilised for industrial-scale productions. However, PLA is expensive compared to starch and takes longer to decompose fully. Blending starch with biodegradable polymers (i.e. PLA/PVA) [91,92] as well as adding multiple fillers with LNPs such as Nanocrystalline cellulose [93] could further improve the biocomposite properties.

## 4. Conclusions

LNPs can be obtained from the EFB-origin lignin via one-step ultrasonication with an average particle size of about 220 nm. The isolated LNPs showed no significant change in structure, as suggested by FTIR results. In addition, LNPs showed improvement in $T_g$ (LNPs: 156 °C, lignin: 154 °C) and $T_{max}$ (LNPs: 285 °C, lignin: 229 °C), suggesting the enhancement of thermal performance. LNPs were found to be stable for a week at pH 4.5–9.0 and salt concentration up to 100 mM. Moreover, LNPs at pH 7 showed negligible change in $D_H$ and zeta potential after being stored for three months. The process involves only water as the suspension medium demonstrated a facile and environmentally benign approach to producing LNPs. On the other hand, LNPs were used to reinforce starch films. It showed better thermal and mechanical performance and a higher hydrophobicity level than lignin composites and neat film. Given their biodegradable nature, these composites could be further improved as a green alternative for petroleum-derived food packaging material. In future studies, it is suggested to examine the possibility of sonicating the wet lignin (lignin before drying) to produce LNPs to reduce the sonication time further. Also, improving the initial lignin concentration (current study 0.5 wt%) would be beneficial to scale up the ultrasonication process, and studies on LNPs toxicology may be necessary to utilise LNPs composite in food packing.

## Summary

Starch composites reinforced with lignin nanoparticles isolated from oil palm empty fruit bunch showed improved mechanical, thermal, and hydrophobic performance.

## Declaration of Competing Interest

The authors declare no competing financial interest.

## Data availability

No data was used for the research described in the article.

## Supplementary materials

Supplementary material associated with this article can be found, in the online version, at doi:10.1016/j.scca.2022.100011.

## References

[1] P. Kowalczyk, B. Ligas, D. Skrzypczak, K. Mikula, G. Izydorczyk, A. Witek-Krowiak, K. Moustakas, K. Chojnacka, Biosorption as a method of biowaste valorization to feed additives: RSM optimization, Environ. Pollut. (2020), doi:10.1016/j.envpol.2020.115937.
[2] E. Derman, R. Abdulla, H. Marbawi, M.K. Sabullah, Oil palm empty fruit bunches as a promising feedstock for bioethanol production in Malaysia, Renew. Energy (2018), doi:10.1016/j.renene.2018.06.003.
[3] C.S. Goh, K.T. Tan, K.T. Lee, S. Bhatia, Bio-ethanol from lignocellulose: status, perspectives and challenges in Malaysia, Bioresour. Technol. (2010), doi:10.1016/j.biortech.2009.08.080.
[4] Y.L. Chiew, S. Shimada, Current state and environmental impact assessment for utilizing oil palm empty fruit bunches for fuel, fiber and fertilizer - A case study of Malaysia, Biomass. Bioenergy (2013), doi:10.1016/j.biombioe.2013.01.012.
[5] R.J. Bouza, Z. Gu, J.H. Evans, Screening conditions for acid pretreatment and enzymatic hydrolysis of empty fruit bunches, Ind. Crops Prod. (2016), doi:10.1016/j.indcrop.2016.01.041.
[6] X.J. Lee, L.Y. Lee, B.Y.Z. Hiew, S. Gan, S. Thangalazhy-Gopakumar, H.K. Ng, Valorisation of oil palm wastes into high yield and energy content biochars via slow pyrolysis: multivariate process optimisation and combustion kinetic studies, Mater. Sci. Energy Technol. (2020), doi:10.1016/j.mset.2020.06.006.
[7] Saifullah Mahidin, Hamdani Erdiwansyah, Hisbullah, A.P. Hayati, M. Zhafran, M.A. Sidiq, A. Rinaldi, B. Fitria, R. Tarisma, Y. Bindar, Analysis of power from palm oil solid waste for biomass power plants: a case study in Aceh Province, Chemosphere (2020), doi:10.1016/j.chemosphere.2020.126714.
[8] A. Tursi, A review on biomass: importance, chemistry, classification, and conversion, Biofuel Res. J. (2019), doi:10.18331/BRJ2019.6.2.3.
[9] P. Vaskan, E.R. Pachón, E. Gnansounou, Techno-economic and life-cycle assessments of biorefineries based on palm empty fruit bunches in Brazil, J. Clean. Prod. (2018), doi:10.1016/j.jclepro.2017.07.218.
[10] A.A. Kamoldeen, C.K. Lee, W.N. Wan Abdullah, C.P. Leh, Enhanced ethanol production from mild alkali-treated oil-palm empty fruit bunches via co-fermentation of glucose and xylose, Renew. Energy 107 (2017) 113–123, doi:10.1016/j.renene.2017.01.039.
[11] A.A. Al-Dulaimi, W.D. Wanrosli, Isolation and characterization of nanocrystalline cellulose from totally chlorine free oil palm empty fruit bunch pulp, J. Polym. Environ. 25 (2017) 192–202, doi:10.1007/s10924-016-0798-z.
[12] M.L. Foo, C.R. Tan, P.D. Lim, C.W. Ooi, K.W. Tan, I.M.L. Chew, Surface-modified nanocrystalline cellulose from oil palm empty fruit bunch for effective binding of curcumin, Int. J. Biol. Macromol. 138 (2019) 1064–1071, doi:10.1016/j.ijbiomac.2019.07.035.

[13] M.N.M. Ibrahim, A. Iqbal, C.C. Shen, S.A. Bhawani, F. Adam, Synthesis of lignin based composites of TiO2 for potential application as radical scavengers in sunscreen formulation, BMC Chem. (2019), doi:10.1186/s13065-019-0537-3.
[14] R. Bhat, H.P.S.A. Khalil, A.A. Karim, Exploring the antioxidant potential of lignin isolated from black liquor of oil palm waste, C. R. Biol. (2009), doi:10.1016/j.crvi.2009.05.004.
[15] Y. Meliana, A.H. Setiawan, Antioxidant activity of lignin phenolic compounds as by-product of pretreatment process of bioethanol production from empty fruits palm bunch, in: AIP Conference Proceedings, 2016, doi:10.1063/1.4941893.
[16] E. Akbarzadeh, M.N.M. Ibrahim, A.A. Rahim, Corrosion inhibition of mild steel in near neutral solution by Kraft and Soda lignins extracted from oil palm empty fruit bunch, Int. J. Electrochem. Sci. 6 (2011) 5396–5416.
[17] M.N.M. Ibrahim, W.S.W. Ngah, M.S. Norliyana, W.R.W. Daud, Copper(II) biosorption on soda lignin from oil palm empty fruit bunches (EFB), Clean (Weinh) (2009), doi:10.1002/clen.200800187.
[18] M.N.M. Ibrahim, A. Ghani, N. Nen, Formulation of lignin phenol formaldehyde resins as a wood adhesive, Malays. J. Anal. Sci. (2007).
[19] H.P.S. Abdul Khalil, M.M. Marliana, A.M. Issam, I.O. Bakare, Exploring isolated lignin material from oil palm biomass waste in green composites, Mater. Des. (2011), doi:10.1016/j.matdes.2011.01.035.
[20] M.N. Garcia Gonzalez, M. Levi, S. Turri, G. Griffini, Lignin nanoparticles by ultrasonication and their incorporation in waterborne polymer nanocomposites, J. Appl. Polym. Sci. 134 (2017), doi:10.1002/app.45318.
[21] J. Rajesh Banu, S. Kavitha, R. Yukesh Kannah, T. Poornima Devi, M. Gunasekaran, S.H. Kim, G. Kumar, A review on biopolymer production via lignin valorization, Bioresour. Technol. (2019), doi:10.1016/j.biortech.2019.121790.
[22] L.E. Low, K.C. Teh, S.P. Siva, I.M.L. Chew, W.W. Mwangi, C.L. Chew, B.-.H. Goh, E.S. Chan, B.T. Tey, Lignin nanoparticles: the next green nanoreinforcer with wide opportunity, Environ. Nanotechnol. Monit. Manag. (2021), doi:10.1016/j.enmm.2020.100398.
[23] K. Ingtipi, V.S. Moholkar, Sonochemically synthesized lignin nanoparticles and its application in the development of nanocomposite hydrogel, in: Materials Today: Proceedings, 2019, doi:10.1016/j.matpr.2019.06.443.
[24] S.S. Nair, S. Sharma, Y. Pu, Q. Sun, S. Pan, J.Y. Zhu, Y. Deng, A.J. Ragauskas, High shear homogenization of lignin to nanolignin and thermal stability of nanolignin-polyvinyl alcohol blends, ChemSusChem 7 (2014) 3513–3520, doi:10.1002/cssc.201402314.
[25] W. Zhao, B. Simmons, S. Singh, A. Ragauskas, G. Cheng, From lignin association to nano-/micro-particle preparation: extracting higher value of lignin, Green Chem. (2016), doi:10.1039/c6gc01813k.
[26] X. He, F. Luzi, X. Hao, W. Yang, L. Torre, Z. Xiao, Y. Xie, D. Puglia, Thermal, antioxidant and swelling behaviour of transparent polyvinyl (alcohol) films in presence of hydrophobic citric acid-modified lignin nanoparticles, Int. J. Biol. Macromol. (2019), doi:10.1016/j.ijbiomac.2019.01.202.
[27] S.R. Yearla, K. Padmasree, Preparation and characterisation of lignin nanoparticles: evaluation of their potential as antioxidants and UV protectants, J. Exp. Nanosci. 11 (2016) 289–302, doi:10.1080/17458080.2015.1055842.
[28] K. Shikinaka, M. Nakamura, Y. Otsuka, Strong UV absorption by nanoparticulated lignin in polymer films with reinforcement of mechanical properties, Polymer (Guildf) (2020), doi:10.1016/j.polymer.2020.122254.
[29] X. Zhang, W. Liu, W. Liu, X. Qiu, High performance PVA/lignin nanocomposite films with excellent water vapor barrier and UV-shielding properties, Int. J. Biol. Macromol. (2020), doi:10.1016/j.ijbiomac.2019.09.129.
[30] M. Ago, S. Huan, M. Borghei, J. Raula, E.I. Kauppinen, O.J. Rojas, High-throughput synthesis of lignin particles (~30 nm to ~2 μm) via aerosol flow reactor: size fractionation and utilization in pickering emulsions, ACS Appl. Mater. Interfaces 8 (2016) 23302–23310, doi:10.1021/acsami.6b07900.
[31] S. Lu, D. Yang, M. Wang, M. Yan, Y. Qian, D. Zheng, X. Qiu, Pickering emulsions synergistic-stabilized by amphoteric lignin and SiO2 nanoparticles: stability and pH-responsive mechanism, Colloids Surf. A Physicochem. Eng. Asp. (2020), doi:10.1016/j.colsurfa.2019.124158.
[32] Y. Qian, X. Zhong, Y. Li, X. Qiu, Fabrication of uniform lignin colloidal spheres for developing natural broad-spectrum sunscreens with high sun protection factor, Ind. Crops Prod. 101 (2017) 54–60, doi:10.1016/j.indcrop.2017.03.001.
[33] L. Dai, R. Liu, L.Q. Hu, Z.F. Zou, C.L. Si, Lignin nanoparticle as a novel green carrier for the efficient delivery of resveratrol, ACS Sustain. Chem. Eng. 5 (2017) 8241–8249, doi:10.1021/acssuschemeng.7b01903.
[34] B. Del Saz-Orozco, M. Oliet, M.V. Alonso, E. Rojo, F. Rodríguez, Formulation optimization of unreinforced and lignin nanoparticle-reinforced phenolic foams using an analysis of variance approach, Compos. Sci. Technol. 72 (2012) 667–674, doi:10.1016/j.compscitech.2012.01.013.
[35] S.M. Roopan, An overview of natural renewable bio-polymer lignin towards nano and biotechnological applications, Int. J. Biol. Macromol. (2017), doi:10.1016/j.ijbiomac.2017.05.103.
[36] S. Shankar, J.W. Rhim, K. Won, Preparation of poly(lactide)/lignin/silver nanoparticles composite films with UV light barrier and antibacterial properties, Int. J. Biol. Macromol. 107 (2018) 1724–1731, doi:10.1016/j.ijbiomac.2017.10.038.
[37] W. Yang, J.M. Kenny, D. Puglia, Structure and properties of biodegradable wheat gluten bionanocomposites containing lignin nanoparticles, Ind. Crops Prod. 74 (2015) 348–356, doi:10.1016/j.indcrop.2015.05.032.
[38] W. Yang, J.S. Owczarek, E. Fortunati, M. Kozanecki, A. Mazzaglia, G.M. Balestra, J.M. Kenny, L. Torre, D. Puglia, Antioxidant and antibacterial lignin nanoparticles in polyvinyl alcohol/chitosan films for active packaging, Ind. Crops Prod. (2016), doi:10.1016/j.indcrop.2016.09.061.
[39] Y. Qian, Y. Deng, X. Qiu, H. Li, D. Yang, Formation of uniform colloidal spheres from lignin, a renewable resource recovered from pulping spent liquor, Green Chem. 16 (2014) 2156–2163, doi:10.1039/c3gc42131g.
[40] M. Lievonen, J.J. Valle-Delgado, M.L. Mattinen, E.L. Hult, K. Lintinen, M.A. Kostiainen, A. Paananen, G.R. Szilvay, H. Setälä, M. Österberg, A simple process for lignin nanoparticle preparation, Green Chem. 18 (2016) 1416–1422, doi:10.1039/c5gc01436k.
[41] Yu Chen, X. Gong, G. Yang, Q. Li, N. Zhou, Preparation and characterization of a nanolignin phenol formaldehyde resin by replacing phenol partially with lignin nanoparticles, RSC Adv. (2019), doi:10.1039/c9ra04827h.
[42] C. Frangville, M. Rutkevičius, A.P. Richter, O.D. Velev, S.D. Stoyanov, V.N. Paunov, Fabrication of environmentally biodegradable lignin nanoparticles, ChemPhysChem 13 (2012) 4235–4243, doi:10.1002/cphc.201200537.
[43] A.P. Richter, J.S. Brown, B. Bharti, A. Wang, S. Gangwal, K. Houck, E.A. Cohen Hubal, V.N. Paunov, S.D. Stoyanov, O.D. Velev, An environmentally benign antimicrobial nanoparticle based on a silver-infused lignin core, Nat. Nanotechnol. 10 (2015) 817–823, doi:10.1038/nnano.2015.141.
[44] C. Abbati De Assis, L.G. Greca, M. Ago, M.Y. Balakshin, H. Jameel, R. Gonzalez, O.J. Rojas, Techno-economic assessment, scalability, and applications of aerosol lignin micro- and nanoparticles, ACS Sustain. Chem. Eng. 6 (2018) 11853–11868, doi:10.1021/acssuschemeng.8b02151.
[45] T.V. Lourencon, L.G. Greca, D. Tarasov, M. Borrega, T. Tamminen, O.J. Rojas, M.Y. Balakshin, Lignin-first integrated hydrothermal treatment (HTT) and synthesis of low-cost biorefinery particles, ACS Sustain. Chem. Eng. (2020), doi:10.1021/acssuschemeng.9b06511.
[46] Ying Chen, K. Zheng, L. Niu, Y. Zhang, Y. Liu, C. Wang, F. Chu, Highly mechanical properties nanocomposite hydrogels with biorenewable lignin nanoparticles, Int. J. Biol. Macromol. (2019), doi:10.1016/j.ijbiomac.2019.01.099.
[47] I.A. Gilca, V.I. Popa, C. Crestini, Obtaining lignin nanoparticles by sonication, Ultrason. Sonochem. 23 (2015) 369–375, doi:10.1016/j.ultsonch.2014.08.021.
[48] D. Yiamsawas, G. Baier, E. Thines, K. Landfester, F.R. Wurm, Biodegradable lignin nanocontainers, RSC Adv. 4 (2014) 11661–11663, doi:10.1039/c3ra47971d.
[49] Y. Qian, Q. Zhang, X. Qiu, S. Zhu, CO2-responsive diethylaminoethyl-modified lignin nanoparticles and their application as surfactants for CO2/N2-switchable Pickering emulsions, Green Chem. 16 (2014) 4963–4968, doi:10.1039/c4gc01242a.
[50] J. Sameni, S. Krigstin, S.A. Jaffer, M. Sain, Preparation and characterization of biobased microspheres from lignin sources, Ind. Crops Prod. 117 (2018) 58–65, doi:10.1016/j.indcrop.2018.02.078.
[51] I.A. Gilca, V.I. Popa, C. Crestini, Obtaining lignin nanoparticles by sonication, Ultrason. Sonochem. 23 (2015) 369–375, doi:10.1016/j.ultsonch.2014.08.021.
[52] S.H. Sekeri, M.N.M. Ibrahim, K. Umar, A.A. Yaqoob, M.N. Azmi, M.H. Hussin, M.B.H. Othman, M.F.I.A. Malik, Preparation and characterization of nanosized lignin from oil palm (Elaeis guineensis) biomass as a novel emulsifying agent, Int. J. Biol. Macromol. (2020), doi:10.1016/j.ijbiomac.2020.08.181.
[53] A.A. Yaqoob, S.H. Sekeri, M.B.H. Othman, M.N.M. Ibrahim, Z.H. Feizi, Thermal degradation and kinetics stability studies of oil palm (Elaeis Guineensis) biomass-derived lignin nanoparticle and its application as an emulsifying agent, Arab. J. Chem. 14 (2021), doi:10.1016/j.arabjc.2021.103182.
[54] S. Rizal, T. Alfatah, H.P.S. Abdul Khalil, E.B. Yahya, C.K. Abdullah, E.M. Mistar, I. Ikramullah, R. Kurniawan, R.D. Bairwan, Enhanced functional properties of bioplastic films using lignin nanoparticles from oil palm-processing residue, Polymers (Basel) 14 (2022) 5126, doi:10.3390/polym14235126.
[55] M.L. Foo, C.W. Ooi, K.W. Tan, I.M.L. Chew, A step closer to sustainable industrial production: tailor the properties of nanocrystalline cellulose from oil palm empty fruit bunch, J. Environ. Chem. Eng. (2020), doi:10.1016/j.jece.2020.104058.
[56] M.Y. Balakshin, E.A. Capanema, Comprehensive structural analysis of biorefinery lignins with a quantitative 13C NMR approach, RSC Adv. 5 (2015) 87187–87199, doi:10.1039/c5ra16649g.
[57] R. Sun, J. Tomkinson, J. Bolton, Effects of precipitation pH on the physico-chemical properties of the lignins isolated from the black liquor of oil palm empty fruit bunch fibre pulping, Polym. Degrad. Stab. (1999), doi:10.1016/S0141-3910(98)00091-3.
[58] N.G. Özcan-Taşkin, G. Padron, A. Voelkel, Effect of particle type on the mechanisms of break up of nanoscale particle clusters, Chem. Eng. Res. Des. 87 (2009) 468–473, doi:10.1016/j.cherd.2008.12.012.
[59] Y. Kim, J. Suhr, H.-.W. Seo, H. Sun, S. Kim, I.-.K. Park, S.-.H. Kim, Y. Lee, K.-.J. Kim, J.-.D. Nam, All Biomass and UV Protective Composite Composed of Compatibilized Lignin and Poly (Lactic-acid), Sci. Rep. 7 (2017), doi:10.1038/srep43596.
[60] B. Wang, X.J. Shen, J.L. Wen, L. Xiao, R.C. Sun, Evaluation of organosolv pretreatment on the structural characteristics of lignin polymers and follow-up enzymatic hydrolysis of the substrates from Eucalyptus wood, Int. J. Biol. Macromol. 97 (2017) 447–459, doi:10.1016/j.ijbiomac.2017.01.069.
[61] M.N. Garcia Gonzalez, M. Levi, S. Turri, G. Griffini, Lignin nanoparticles by ultrasonication and their incorporation in waterborne polymer nanocomposites, J. Appl. Polym. Sci. 134 (2017) 1–10, doi:10.1002/app.45318.
[62] F. Xu, D. Wang, Analysis of lignocellulosic biomass using infrared methodology, Pretreat. Biomass (2014) 7–25, doi:10.1016/B978-0-12-800080-9.00002-5.
[63] Y. Deng, X. Feng, M. Zhou, Y. Qian, H. Yu, X. Qiu, Investigation of aggregation and assembly of alkali lignin using iodine as a probe, Biomacromolecules 12 (2011) 1116–1125, doi:10.1021/bm101449b.
[64] M.N. M Ibrahim, N. Zakaria, C.S. Sipaut, O. Sulaiman, R. Hashim, Chemical and thermal properties of lignins from oil palm biomass as a substitute for phenol in a phenol formaldehyde resin production, Carbohydr. Polym. (2011), doi:10.1016/j.carbpol.2011.04.018.
[65] J.D. Coral Medina, A.L. Woiciechowski, A. Zandona Filho, L. Bissoqui, M.D. Noseda, L.P. de Souza Vandenberghe, S.F. Zawadzki, C.R. Soccol, Biological activ-

ities and thermal behavior of lignin from oil palm empty fruit bunches as potential source of chemicals of added value, Ind. Crops Prod. (2016), doi:10.1016/j.indcrop.2016.09.046.
[66] S. Sen, S. Patil, D.S. Argyropoulos, Thermal properties of lignin in copolymers, blends, and composites: a review, Green Chem. (2015), doi:10.1039/c5gc01066g.
[67] M.G. Alriols, A. Tejado, M. Blanco, I. Mondragon, J. Labidi, Agricultural palm oil tree residues as raw material for cellulose, lignin and hemicelluloses production by ethylene glycol pulping process, Chem. Eng. J. 148 (2009) 106–114, doi:10.1016/j.cej.2008.08.008.
[68] R.C. Sun, Q. Lu, X.F. Sun, Physico-chemical and thermal characterization of lignins from Caligonum monogoliacum and Tamarix spp, Polym. Degrad. Stab. 72 (2001) 229–238, doi:10.1016/S0141-3910(01)00023-4.
[69] J.C. Domínguez, M. Oliet, M.V. Alonso, M.A. Gilarranz, F. Rodríguez, Thermal stability and pyrolysis kinetics of organosolv lignins obtained from Eucalyptus globulus, Ind. Crops Prod. 27 (2008) 150–156, doi:10.1016/j.indcrop.2007.07.006.
[70] O.U. Rahman, S. Shi, J. Ding, D. Wang, S. Ahmad, H. Yu, Lignin nanoparticles: synthesis, characterization and corrosion protection performance, New J. Chem. 42 (2018) 3415–3425, doi:10.1039/c7nj04103a.
[71] D. Narapakdeesakul, W. Sridach, T. Wittaya, Recovery, characteristics and potential use as linerboard coatings material of lignin from oil palm empty fruit bunches' black liquor, Ind. Crops Prod. (2013), doi:10.1016/j.indcrop.2013.07.011.
[72] A. García, M.G. Alriols, R. Llano-Ponte, J. Labidi, Ultrasound-assisted fractionation of the lignocellulosic material, Bioresour. Technol. 102 (2011) 6326–6330, doi:10.1016/j.biortech.2011.02.045.
[73] D. Narapakdeesakul, W. Sridach, T. Wittaya, Recovery, characteristics and potential use as linerboard coatings material of lignin from oil palm empty fruit bunches' black liquor, Ind. Crops Prod. 50 (2013) 8–14, doi:10.1016/j.indcrop.2013.07.011.
[74] C.T. Moynihan, A.J. Easteal, J. Wilder, J. Tucker, Dependence of the glass transition temperature on heating and cooling rate, J. Phys. Chem. (1974), doi:10.1021/j100619a008.
[75] S.J. Juikar, N. Vigneshwaran, Extraction of nanolignin from coconut fibers by controlled microbial hydrolysis, Ind. Crops Prod. 109 (2017) 420–425, doi:10.1016/j.indcrop.2017.08.067.
[76] A.P. Richter, B. Bharti, H.B. Armstrong, J.S. Brown, D. Plemmons, V.N. Paunov, S.D. Stoyanov, O.D. Velev, Synthesis and characterization of biodegradable lignin nanoparticles with tunable surface properties, Langmuir 32 (2016) 6468–6477, doi:10.1021/acs.langmuir.6b01088.
[77] M.B. Agustin, P.A. Penttilä, M. Lahtinen, K.S. Mikkonen, Rapid and direct preparation of lignin nanoparticles from alkaline pulping liquor by mild ultrasonication, ACS Sustain. Chem. Eng. (2019), doi:10.1021/acssuschemeng.9b05445.
[78] H.J. Choi, Effect of Mg-sericite flocculant for treatment of brewery wastewater, Appl. Clay Sci. 115 (2015) 145–149, doi:10.1016/j.clay.2015.07.037.
[79] J. Sameni, S. Krigstin, S.A. Jaffer, M. Sain, Preparation and characterization of biobased microspheres from lignin sources, Ind. Crops Prod. 117 (2018) 58–65, doi:10.1016/j.indcrop.2018.02.078.
[80] B. Bharti, J. Meissner, S.H.L. Klapp, G.H. Findenegg, Bridging interactions of proteins with silica nanoparticles: the influence of pH, ionic strength and protein concentration, Soft Matter 10 (2014) 718–728, doi:10.1039/c3sm52401a.
[81] Y. Peng, S.S. Nair, H. Chen, N. Yan, J. Cao, Effects of lignin content on mechanical and thermal properties of polypropylene composites reinforced with micro particles of spray dried cellulose nanofibrils, ACS Sustain. Chem. Eng. 6 (2018) 11078–11086, doi:10.1021/acssuschemeng.8b02544.
[82] P. Balakrishnan, M.S. Sreekala, V.G. Geethamma, N. Kalarikkal, V. Kokol, T. Volova, S. Thomas, Physicochemical, mechanical, barrier and antibacterial properties of starch nanocomposites crosslinked with pre-oxidised sucrose, Ind. Crops Prod. (2019), doi:10.1016/j.indcrop.2019.01.007.
[83] A. Owais, M. Khaled, B.S. Yilbas, Hydrophobicity and surface finish, Compreh. Mater. Finish. (2016), doi:10.1016/B978-0-12-803581-8.09172-4.
[84] T. AbdulRasheed-Adeleke, E.C. Egwim, E.R. Sadiku, S.S. Ochigbo, Optimisation of lignin–cellulose nanofiber-filled thermoplastic starch composite film production for potential application in food packaging, Molecules 27 (2022) 7708, doi:10.3390/molecules27227708.
[85] X. Wang, H. Sun, H. Bai, L.P. Zhang, Thermal, mechanical, and degradation properties of nanocomposites prepared using lignin-cellulose nanofibers and poly(lactic acid), Bioresources 9 (2014), doi:10.15376/biores.9.2.3211-3224.
[86] C. Wang, S.S. Kelley, R.A. Venditti, Lignin-based thermoplastic materials, ChemSusChem 9 (2016), doi:10.1002/cssc.201501531.
[87] W. Yang, H. Ding, G. Qi, C. Li, P. Xu, T. Zheng, X. Zhu, J.M. Kenny, D. Puglia, P. Ma, Highly transparent PVA/nanolignin composite films with excellent UV shielding, antibacterial and antioxidant performance, React. Funct. Polym. 162 (2021), doi:10.1016/j.reactfunctpolym.2021.104873.
[88] W. Yang, E. Fortunati, F. Dominici, G. Giovanale, A. Mazzaglia, G.M. Balestra, J.M. Kenny, D. Puglia, Synergic effect of cellulose and lignin nanostructures in PLA based systems for food antibacterial packaging, Eur. Polym. J. 79 (2016) 1–12, doi:10.1016/j.eurpolymj.2016.04.003.
[89] M. Parit, P. Saha, V.A. Davis, Z. Jiang, Transparent and homogenous cellulose nanocrystal/lignin UV-protection films, ACS Omega (2018), doi:10.1021/acsomega.8b01345.
[90] P. G, S. AS, J.S. Jayan, A. Raman, A. Saritha, Lignin based nanocomposites: synthesis and applications, Process Saf. Environ. Protect. (2021), doi:10.1016/j.psep.2020.11.017.
[91] S. Ni, H. Bian, Y. Zhang, Y. Fu, W. Liu, M. Qin, H. Xiao, Starch-based composite films with enhanced hydrophobicity, thermal stability, and uv-shielding efficacy induced by lignin nanoparticles, Biomacromolecules 23 (2022), doi:10.1021/acs.biomac.1c01288.
[92] J.F. Zhang, X. Sun, Mechanical properties of poly(lactic acid)/starch composites compatibilized by maleic anhydride, Biomacromolecules 5 (2004), doi:10.1021/bm0400022.
[93] U.P. Perera, M.L. Foo, I. Mei, L. Chew, Application of nanolignin and nanocrystalline cellulose isolated from palm oil empty fruit bunch as reinforcing agents in starch biocomposite, Environ. & Health 13 (2022) 1–12, doi:10.5366/jope.2022.01.